Robust Full Waveform Inversion of Surface Waves

Isabella Masoni, Total E&P, Univ. Grenoble Alpes, R. Brossier, Univ. Grenoble Alpes, J. L. Boelle, Total E&P, J. Virieux, Univ. Grenoble Alpes*

SUMMARY

To mitigate the probem of cycle-skipping for FWI using surface waves on an exploration scale, more robust misfit functions based on alternative data domains have recently been proposed. In this study simple synthetic inversion tests are used to investigate the more robust behavior of these approaches compared to the classical FWI approach. Misfit functions in the $\omega - p$ and the $\omega - k$ domains are shown to be more robust in the presence of cycle-skipping for very simple to complex laterally varying models.

INTRODUCTION

The construction of subsurface velocity models is an ongoing issue for oil & gas exploration. In complex terrain, such as regions with topography or laterally varying shallow structures, the imaging of deeper exploration targets may still be problematic due to the presence of groundroll. In such cases, an innovative characterization of near surface properties is needed, and the inversion of surface waves, which sample this shallow zone, appears to be essential to image deeper lying targets. Using Full Waveform Inversion (FWI) as a high-resolution imaging technique, allows to extend beyond the 1D limitations of more conventional surface wave imaging methods.

THEORY

A key feature of FWI is the misfit function that classically considers the point-to-point difference between the observed data and the calculated data, to provide high-resolution imaging using a local optimization approach. If the initial data do not predict the observed data with an error smaller than half a period, the optimization may get stuck in a local minimum due to cycle-skipping (Mulder and Plessix, 2008).

The generic FWI formalism does not rely on a specific wave type. In practice however, success with FWI has mainly exploited body waves under an acoustic approximation of wave-propagation. Although some elastic FWI applications have been performed using body waves, the use of surface waves is still challenging (Brossier et al., 2009). Yet it appears that if the kinematics predicted by the initial model are close to the observed data, the diffraction of surface waves can provide useful information (Bretaudeau et al., 2013).

In the case of slow surface waves propagating in the low velocity medium of the near surface, finding a sufficiently accurate initial model is mandatory for avoiding local minima. Array processing and lateral coherency of seismic arrivals could be exploited to mitigate cycle-skipping, and more robust misfit functions have been proposed with the aim to tackle this issue (Masoni et al., 2013; Perez Solano et al., 2013).

Alternative misfit functions

The FWI misfit function is often defined as the L2 norm of the difference between the observed and the calculated data in a given domain, classically in $t - x$, leading to

$$C_{t,x} = \frac{1}{2}\left(\mathbf{d_{obs}}(t,x)\right) - \left(\mathbf{d_{cal}}(t,x)\right)^2. \tag{1}$$

Alternative data domains may provide more robustness and help approach the problem from a different point of view. In this study, transformations associated with the $\tau - p$, $\omega - p$ and $\omega - k$ domains are considered, giving the following functions

$$C_{\tau,p} = \frac{1}{2}\left(\mathbf{d_{obs}}(\tau,p)\right) - \left(\mathbf{d_{cal}}(\tau,p)\right)^2, \tag{2}$$

$$C_{\omega,p} = \frac{1}{2}\left(|\mathbf{d_{obs}}(\omega,p))| - |\left(\mathbf{d_{cal}}(\omega,p)|\right)^2, \tag{3}$$

$$C_{\omega,k} = \frac{1}{2}\left(|\mathbf{d_{obs}}(\omega,k))| - |\left(\mathbf{d_{cal}}(\omega,k)|\right)^2. \tag{4}$$

Applying a linear moveout (LMO) to obtain data in the $\tau - p$ and $\omega - p$ domains, and separating events by their slowness, might allow the extraction of kinematic information more robustly. Furthermore the stacking involved in the transformation may also make the misfit function more efficient in the presence of noise. Projecting data to the $\omega - p$ and $\omega - k$ domains through the use of a Fourier transform may help to explicitly consider frequency dependent dispersion effects. In the frequency domain, the modulus of the data is considered. This may make the misfit function insensitive to the phase of the source wavelet, but should not limit the capacity of fitting the kinematic properties contained in the data.

Gradient formulation

To minimize the misfit function and update the model, the gradient needs to be computed. The adjoint-state method (Chavent, 1974; Plessix, 2006) is often used in FWI, as it is more efficient than computing Fréchet derivatives. The adjoint states correspond to a back-propagated field, the source of which is directly linked to the choice of the misfit function. The development of the gradient expression with a new adjoint source formulation for the alternative misfit functions is described in more detail in Masoni et al. (2014).

Derived from a Lagrangian formalism, the gradient for the difference-based misfit in the $\tau - p$ domain is

$$\frac{\partial \mathscr{L}}{\partial m} = [\frac{\partial A(m)}{\partial m}\mathbf{u}(t)]^{\dagger} A(m)^{-\dagger} R^{\dagger} \frac{1}{rms} T^{\dagger} \Big(\left(\mathbf{d_{obs}}(\tau,p) - \mathbf{d_{cal}}(\tau,p)\right)\Big), \tag{5}$$

where $T^{\dagger} = \sum_p (\tau = t - px)$ is defined.

DOI http://dx.doi.org/10.1190/segam2014-1077.1

The projection operator R extracts the wavefield $\mathbf{u}(t)$ at the receiver positions, A represents the forward problem operator, $\mathbf{s}(t)$ the source, and the subscript N implies data normalized by the *rms* of each trace. This expression shows that all the steps considered to compute the misfit are present in the adjoint source through their adjoint operator, allowing a physical understanding of the adjoint source.

Appropriate formulations of the gradients for the $\omega - p$ and $\omega - k$ domains are also derived (Equations 6 and 7). In these domains the adjoint effect of taking the modulus of the data adds a multiplication by the phase of the data. For the for the $\omega - p$ domain the gradient expression is

$$\frac{\partial \mathscr{L}}{\partial m} = [\frac{\partial A(m)}{\partial m}\mathbf{u}(t)]^{\dagger} A(m)^{-\dagger} R^{\dagger} \frac{1}{rms} T_1^{\dagger} \left(T_2^{\dagger}\left(\left(|\mathbf{d_{obs}}(\omega,p)| - |\mathbf{d_{cal}}(\omega,p)|\right)\frac{\mathbf{d_{cal}}(\omega,p)}{|\mathbf{d_{cal}}(\omega,p)|}\right)\right), \quad (6)$$

where $T_1^{\dagger} = \sum_p (\tau = t - px)$ and $T_2^{\dagger} = \sum_\omega e^{i\omega t}$,

and for the $\omega - k$ domain the gradient is

$$\frac{\partial \mathscr{L}}{\partial m} = [\frac{\partial A(m)}{\partial m}\mathbf{u}(t)]^{\dagger} A(m)^{-\dagger} R^{\dagger} \frac{1}{rms} T_1^{\dagger} \left(T_2^{\dagger}\left(\left(|\mathbf{d_{obs}}(\omega,k)| - |\mathbf{d_{cal}}(\omega,k)|\right)\frac{\mathbf{d_{cal}}(\omega,k)}{|\mathbf{d_{cal}}(\omega,k)|}\right)\right), \quad (7)$$

where $T_1^{\dagger} = \sum_k e^{ikx}$ and $T_2^{\dagger} = \sum_\omega e^{i\omega t}$.

Again the components of the gradient mirror the steps taken to compute the misfit in the relevant domains, and the Fourier transform applied to the data results in an inverse Fourier transform applied to the adjoint source. Although the new adjoint source expressions seem more complicated than in the classical FWI formulation, they only have a minor additional computational cost compared to the wave-propagation modeling.

SYNTHETIC TESTS

Simple inversion tests are used to compare the robustness of the alternative FWI approaches presented. To compute the synthetic data, 2D elastic wave propagation is simulated using a finite difference method. The focus of these tests is on the exploitation of the surface waves, which dominate the data with the highest amplitude and are therefore also the main wavefield component driving misfit minimization.

Homogeneous model

The first and most simplest test consists of a homogeneous velocity model with shear velocity $Vs = 1200\ m/s$ (Figure 2a). The Vp and density parameters are also homogeneous, and therefore no dispersion is present in the data, as shown in Figure 1a.

A land streamer-like acquisition is used, consisting of 16 sources evenly spaced at 25 m intervals, each with a line of 36 receivers on the right-hand-side of the source that have a spacing of 6.25 m. The receivers are both z and x component, and both

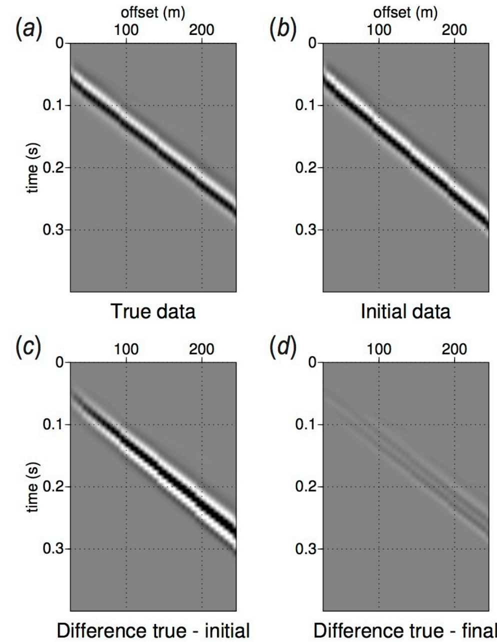

Figure 1: Synthetic data derived from the true homogeneous model (a), the initial model (b), the difference between true and initial (c), and the difference between true and the final data from the result of FWI in the $\omega - p$ domain (d). The final data after FWI in the $\omega - p$ domain is almost indistinguishable from the true data at this scale and is therefore not plotted.

are used in the FWI. The source is a vertical Ricker wavelet of 10 Hz peak frequency, and is assumed to be known in the inversion. The first source location is at 0 m along the horizontal axis of the model and the last source is at a distance of 415 m. As all the model parameters are homogenous, any lateral variations in the inversion results are most likely due to the acquisition and site effects.

The initial model is also homogeneous but with a wrong velocity of $Vs = 1100\ m/s$ (Figure 2b). In the inversion both Vs and Vp are inverted for simultaneously and independently. The initial Vp/Vs ratio is true. However, there is no constrain on this parameter during the inversion. Although this initial model is relatively close to the true model, the small difference in velocity is large enough to create some cycle-skipping at far offset as seen in Figure 1c.

The final Vs result after FWI is shown for each misfit function in Figure 2. The results suggest that FWI using a misfit function in either the $\omega - p$ or $\omega - k$ domain is more robust, and rather successful in recovering the true model. This result is consistent with conclusions from sensitivity tests of these misfit functions (Masoni et al., 2013; Perez Solano et al., 2013). The two results are also very similar to each other, with the only difference perhaps due to sampling issues.

With the classical FWI approach in the $t - x$ domain, as well as with FWI in the $\tau - p$ domain, the velocity in the very near surface is overestimated, and the velocity at depth underesti-

DOI http://dx.doi.org/10.1190/segam2014-1077.1

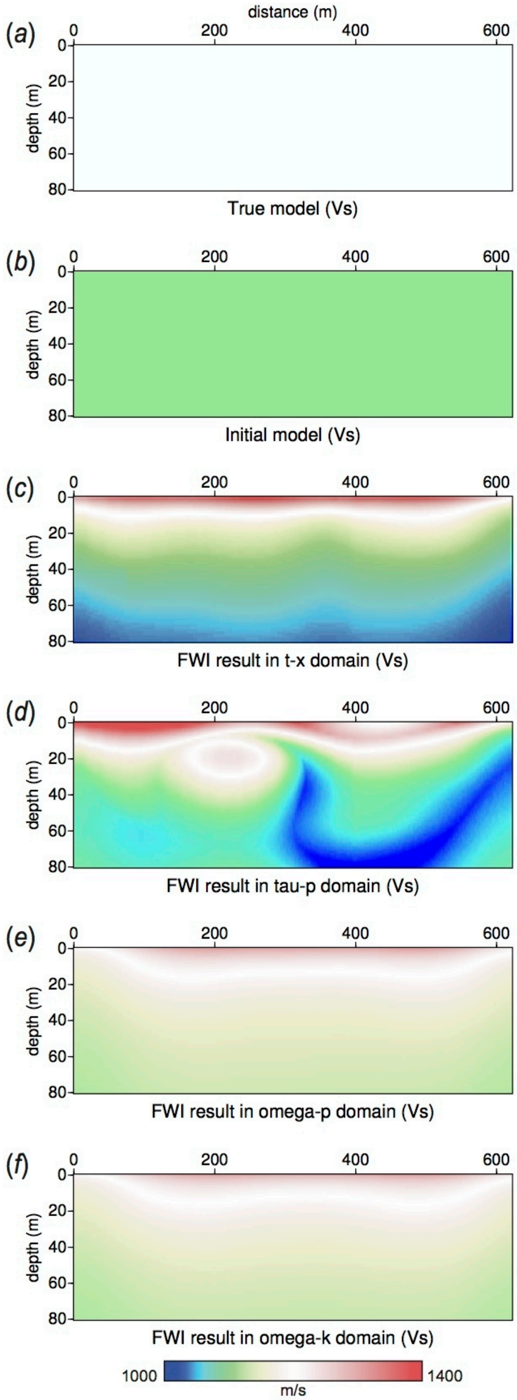

Figure 2: True Vs model used to generate the synthetic data (a); initial Vs model for FWI (b); and the resulting Vs models after FWI in the $t-x$ domain (c), the $\tau-p$ domain (d), the $\omega-p$ domain (e), and the $\omega-k$ domain (f).

mated to compensate. Furthermore for the $\tau-p$ domain, the anomaly on the right hand side of the model may perhaps be explained by the acquisition scheme, as the last source location is at 415 m. The inversion is stuck in a local minimum.

The recovered Vs models also illustrate that the depth sensitivity of the surface waves, which drive the misfit function and the model update, is limited to around the top 40 m of the model. The deeper part of the model is not correctly recovered.

The simultaneaus inversion of the Vp parameter is also equally successful in the $\omega-p$ and $\omega-k$ domains, and the top 40 m of the Vp model is correctly recovered, except for the edges of the model due to a partial acquisition.

Laterally varying model

A second, more complex test is the FWI of a laterally varying two-layer velocity model. In this test, the aim is the reconstruction of a lateral and vertical velocity gradient in the first layer to a depth of 20 m. The second layer is of homogeneous velocity.

The acquisition simulated is a fixed-spread consisting of 24 vertical sources and 48 multi-component receivers evenly spaced on the surface of the 600 m long model. The source is again a vertical Ricker wavelet of 10 Hz peak frequency, and is assumed to be known. The resulting dataset is shown in Figure 3a. The velocity gradient creates very complex surface waves with dispersion effects and higher modes.

In this case, only the Vs parameter is inverted for, since surface waves are most sensitive to it, while Vp and density, are considered as known. The initial model for Vs contains a ho-

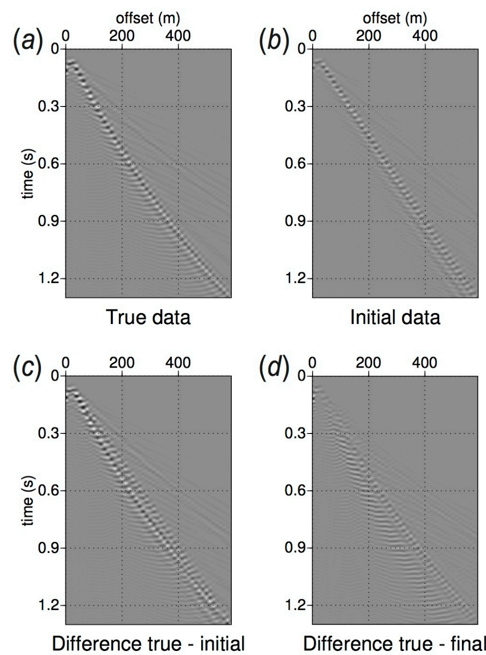

Figure 3: Synthetic data derived from the true laterally varying model (a), the initial model (b), the difference between true and initial (c), and the difference between true and the final data from the result of FWI in the $\omega-k$ domain (d). The final data after FWI in the $\omega-k$ domain is almost indistinguishable from the true data at this scale and is therefore not plotted.

DOI http://dx.doi.org/10.1190/segam2014-1077.1

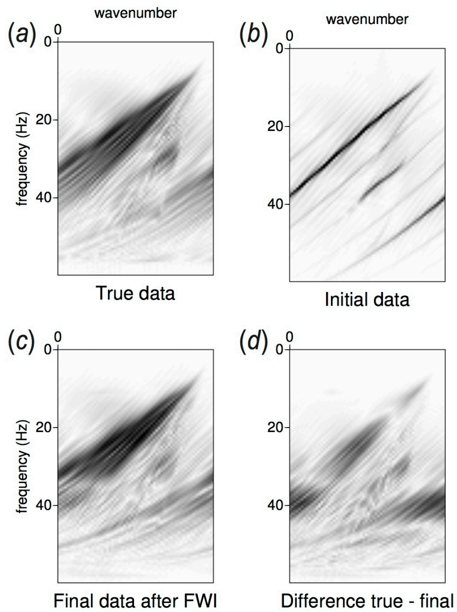

Figure 4: Results for FWI in the $\omega - k$ domain: data for a single source shown in the $\omega - k$ domain for the true model (a), the initial model (b), the final recovered model after FWI (c), and the difference between the true and the final (d).

mogeneous layer at the surface as shown in Figure 5b. The depth of the 1st layer, and the velocity of the second layer is known. The difference between the true data and the initial data is large enough to cause cycle-skipping, especially at mid to long offset, as can be seen in Figure 3c.

For the FWI results using both the $t - x$ and $\tau - p$ misfit functions, no convergence and no updating of the Vs model is observed. The vertical and lateral gradients are instead well recovered by FWI in the $\omega - p$ and the $\omega - k$ domains, as shown in Figures 5c and 5d. The convergence for these two domains has clearly moved in the right direction, despite the cycle skipping present in the data. This stronger robustness may be explained by Figure 4, which displays how the data appear in the $\omega - k$ domain, where the optimization is performed. The initial data are now better embedded in the true data, allowing convergence. The optimization helps decrease the difference between the true data and the final data after FWI in the $\omega - k$ domain, as can be seen in both the typical $t - x$ plot (Figure 3d) as well as directly in the $\omega - k$ domain (Figure 4d), further illustrating the importance of the domain considered.

CONCLUSIONS

In this study, simple synthetic inversion tests are used to investigate FWI with misfit functions in alternative domains compared to the classical FWI approach. Misfits in the $\omega - p$ and the $\omega - k$ domains are shown to be more robust in the inversion of surface waves, where the data is cycle-skipped. The two very different inversion tests suggest that this conclusion is valid for very simple to complex laterally varying models,

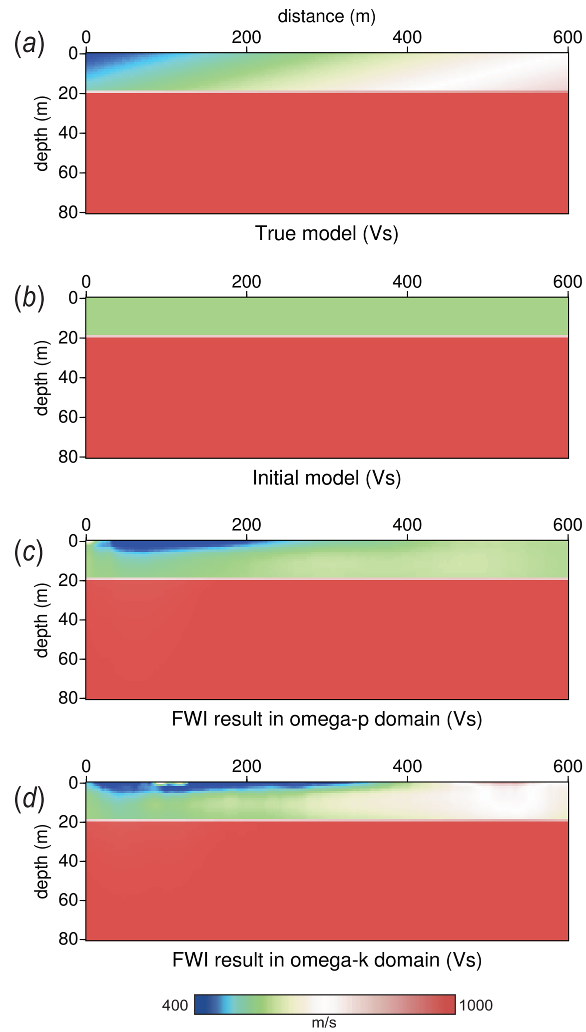

Figure 5: True Vs model used to generate the synthetic data (a); initial Vs model for FWI; and the resulting Vs models after FWI in the $\omega - p$ domain (c), and in the $\omega - k$ domain (d). Convergence in the classical $t - x$ domain and in the $\tau - p$ domain stops after the first iteration without updating the Vs model.

as well as various acquisition schemes. Furthermore, for the simplest inversion test, the Vp parameter is also successfully recovered for the near surface in an inversion mainly driven by surface waves. This leads to promising perspectives for the imaging of near-surface targets, and demands further investigations of the limitations of these more robust FWI approaches.

ACKNOWLEDGMENTS

The authors would like to thank TOTAL E&P for permission to show these results. This work was produced using the CIMENT high-performance computing facilities (Université Grenoble Alpes).

DOI http://dx.doi.org/10.1190/segam2014-1077.1

http://dx.doi.org/10.1190/segam2014-1077.1

EDITED REFERENCES

Note: This reference list is a copy-edited version of the reference list submitted by the author. Reference lists for the 2014 SEG Technical Program Expanded Abstracts have been copy edited so that references provided with the online metadata for each paper will achieve a high degree of linking to cited sources that appear on the Web.

REFERENCES

Bretaudeau, F., R. Brossier, D. Leparoux, O. Abraham, and J. Virieux, 2013, 2D elastic full-waveform imaging of the near surface: Application to synthetic and a physical modeling data sets: Near Surface Geophysics, **11**, 307–316.

Brossier, R., S. Operto, and J. Virieux, 2009, Seismic imaging of complex onshore structures by 2D elastic frequency-domain full-waveform inversion: Geophysics, **74**, no. 6, WCC105–WCC118, http://dx.doi.org/10.1190/1.3215771.

Chavent, G., 1974, Identification of parameter distributed systems, *in* Identification of function parameters in partial differential equations: American Society of Mechanical Engineers, 31–48.

Masoni, I., R. Brossier, J. L. Boelle, and J. Virieux, 2014, Generic gradient expression for robust FWI of surface waves: 76th Annual International Conference and Exhibition, EAGE, Extended Abstracts, E106 01.

Masoni, I., R. Brossier, J. Virieux, and J. Boelle, 2013, Alternative misfit functions for FWI applied to surface waves: 75th Annual International Conference and Exhibition, EAGE, Extended Abstracts, P10 13.

Mulder, W., and R. E. Plessix, 2008, Exploring some issues in acoustic full-waveform inversion: Geophysical Prospecting, **56**, no. 6, 827–841, http://dx.doi.org/10.1111/j.1365-2478.2008.00708.x.

Perez Solano, C., D. Donno, and H. Chauris, 2013, 2D surface-wave inversion in the F-K domain: 75th Annual International Conference and Exhibition, EAGE, Extended Abstracts, Th 10 07.

Plessix, R. E., 2006, A review of the adjoint-state method for computing the gradient of a functional with geophysical applications: Geophysical Journal International, **167**, no. 2, 495–503, http://dx.doi.org/10.1111/j.1365-246X.2006.02978.x.